Linear Trinuclear Pt···Mo−Mo Complexes $[Mo_2PtX_2(pyphos)_2(O_2CR)_2]_2$ (X = Cl, Br, I; R = CH_3, $C(CH_3)_3$; pyphos = 6-(Diphenylphosphino)-2-pyridonate) with an Axial Interaction between the Quadruply Bonded Mo_2 Moiety and the Platinum Atom

Hiroshi Nakano and Akira Nakamura*

Department of Macromolecular Science, Faculty of Science, Osaka University, Toyonaka, Osaka 560, Japan

Kazushi Mashima*

Department of Chemistry, Faculty of Engineering Science, Osaka University, Toyonaka, Osaka 560, Japan

Received August 2, 1995[⊗]

An example of a direct axial interaction of a platinum(II) atom with a Mo_2 core through a uniquely designed tridentate ligand 6-(diphenylphosphino)-2-pyridonate (abbreviated as pyphos) is described. Treatment of $PtX_2(pyphosH)_2$ (**2a**, X = Cl; **2b**, X = Br; **2c**, X = I) with a 1:1 mixture of $Mo_2(O_2CCH_3)_4$ and $[Mo_2(O_2CCH_3)_2(NCCH_3)_6]^{2+}$ (**3a**) in dichloromethane afforded the linear trinuclear complexes $[Mo_2PtX_2(pyphos)_2(O_2CCH_3)_2]_2$ (**4a**, X = Cl; **4b**, X = Br; **4c**, X = I). The reaction of $[Mo_2(O_2CCMe_3)_2(NCCH_3)_4]^{2+}$ (**3b**) with **2a**−**c** in dichloromethane afforded the corresponding pivalato complexes $[Mo_2PtX_2(pyphos)_2(O_2CCMe_3)_2]_2$ (**5a**, X = Cl; **5b**, X = Br; **5c**, X = I), whose bonding nature is discussed on the basis of the data from Raman and electronic spectra as well as cyclic voltammograms. The linear trinuclear structures in **4b** and **5a**−**c** were confirmed by NMR studies and X-ray analyses: **4b**, monoclinic, space group $C2/c$, a = 34.733(4) Å, b = 17.81(1) Å, c = 22.530(5) Å, β = 124.444(8)°, V = 11498(5) Å^3, Z = 8, R = 0.060 for 8659 reflections with $I > 3\sigma(I)$ and 588 parameters; **5a**, triclinic, space group $P\bar{1}$, a = 13.541(3) Å, b = 17.029(3) Å, c = 12.896(3) Å, α = 101.20(2)°, β = 117.00(1)°, γ = 85.47(2)°, V = 2599(1) Å^3, Z = 2, R = 0.050 for 8148 reflections with $I > 3\sigma(I)$ and 604 parameters; **5b**, triclinic, space group $P\bar{1}$, a = 12.211(2) Å, b = 20.859(3) Å, c = 10.478(2) Å, α = 98.88(1)°, β = 112.55(2)°, γ = 84.56(1)°, V = 2433.3(8) Å^3, Z = 2, R = 0.042 for 8935 reflections with $I > 3\sigma(I)$ and 560 parameters; **5c**, monoclinic, space group $P2_1/n$, a = 13.359(4) Å, b = 19.686(3) Å, c = 20.392(4) Å, β = 107.92(2)°, V = 5101(2) Å^3, Z = 4, R = 0.039 for 8432 reflections with $I > 3\sigma(I)$ and 560 parameters.

Introduction

Since the quadruple metal−metal bond containing the δ component was recognized in 1964, the chemistry of multiply bonded bimetal complexes, especially those of group 6 metals and rhenium, has been extensively developed.[1] The interaction of organic axial ligands with a quadruply bonded M_2 moiety has been investigated because this interaction elongates the metal−metal bond distance.[2−4] Recently, Chisholm *et al.* prepared the tetranuclear complex $[Mo_2(O_2CCMe_3)_3]_2(\mu$-2,7-$O_2N_2C_8H_4)$ composed of two quadruply bonded Mo_2 moieties by using a tetradentate 2,7-dioxynaphthyridine ligand.[5] This tetranuclear complex has no direct axial metal−metal interaction between the two Mo_2 moieties, and the oxygen atom of the neighboring μ-carboxylato ligand was found to coordinate at the axial position of the Mo_2 core.

With a unique tridentate ligand, 6-(diphenylphosphino)-2-pyridonate (=pyphos), we prepared the straight linear tetranuclear Pd−Mo−Mo−Pd complex $Mo_2Pd_2Cl_2(pyphos)_4$, in which the four metal atoms are bonded in straight linear fashion.[6] The linear trinuclear Pd···Mo−Mo complex $[Mo_2PdCl_2(pyphos)_2(O_2CCH_3)_2]_2$ (**1**) was also synthesized.[6] As an extension of this work, we investigated the interaction of an Mo_2 core with an axial platinum atom, analogous to the bonding interaction between a molybdenum atom and a platinum atom in some cluster complexes.[7−10] We describe here the syntheses and structures of linear trinuclear Pt···Mo−Mo complexes of formula $[Mo_2PtX_2(pyphos)_2(O_2CR)_2]_2$ [R = CH_3 (**4**), $C(CH_3)_3$ (**5**); X = Cl, Br, I], and the effects on the Mo_2 fragment of this axial interaction.

Results and Discussion

Preparation of $[Mo_2PtX_2(pyphos)_2(O_2CCH_3)_2]_2$ (4) and $[Mo_2PtX_2(pyphos)_2(O_2CCMe_3)_2]_2$ (5). The starting complexes $PtX_2(pyphosH)_2$ (**2a**, X = Cl; **2b**, X = Br; **2c**, X = I) were prepared quantitatively by ligand exchange reactions of PtX_2(cod) (cod = 1,5-cyclooctadiene) with 6-(diphenylphosphino)-2-pyridone (abbreviated as pyphosH). The linear trinuclear Mo_2Pt complex $[Mo_2PtCl_2(pyphos)_2(O_2CCH_3)_2]_2$ (**4a**) was

[⊗] Abstract published in *Advance ACS Abstracts,* May 1, 1996.

(1) Cotton, F. A.; Walton, R. A. *Multiple Bonds between Metal Atoms;* 2nd. ed.; Oxford University Press: Oxford, U.K., 1993.
(2) Cotton, F. A.; Extine, M.; Gage, L. D. *Inorg. Chem.* **1978**, *17*, 172.
(3) Cotton, F. A. *Acc. Chem. Res.* **1978**, *11*, 225.
(4) Cotton, F. A.; Wang, W. *Nouv. J. Chim.* **1984**, *8*, 331.
(5) Cayton, R. H.; Chisholm, M. H.; Huffman, J. C.; Lobkovsky, E. B. *J. Am. Chem. Soc.* **1991**, *113*, 8709.
(6) Mashima, K.; Nakano, H.; Nakamura, A. *J. Am. Chem. Soc.* **1993**, *115*, 11632.
(7) Braunstein, P.; Jud, J.-M.; Dusausoy, Y.; Fischer, J. *Organometallics* **1983**, *2*, 180.
(8) Loeb, S. J.; Taylor, H. A.; Gelmini, L.; Stephan, D. W. *Inorg. Chem.* **1986**, *25*, 1977.
(9) Powell, J.; Couture, C.; Gregg, M. R.; Sawyer, J. F. *Inorg. Chem.* **1989**, *28*, 3437.
(10) Ferrer, M.; Rossell, O.; Seco, M. *J. Chem. Soc., Dalton Trans.* **1989**, 379.

S0020-1669(95)00988-8 CCC: $12.00

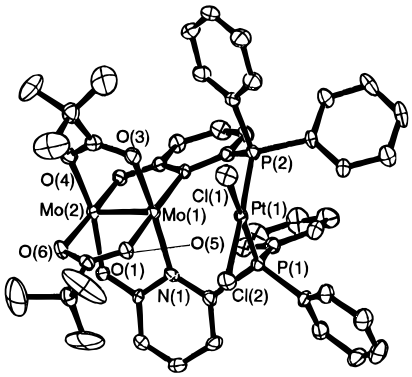

Figure 1. View of the monomeric part of **5a** with labeling scheme. Thermal ellipsoids are drawn at the 30% probability level.

obtained in 56% yield by reaction of **2a** with a dichloromethane solution of a 1:1 mixture of $Mo_2(O_2CCH_3)_4$ and $[Mo_2(O_2CCH_3)_2(NCCH_3)_6]^{2+}$ (**3a**). Reaction of **2a** with **3a** also afforded **4a**, but the yield was poor (5%). Similarly, the complexes $[Mo_2PtBr_2(pyphos)_2(O_2CCH_3)_2]_2$ (**4b**) and $[Mo_2PtI_2(pyphos)_2(O_2CCH_3)_2]_2$ (**4c**) were prepared by reactions with **2b** and **2c**, respectively. Complexes **4a**−**c** have low solubility; therefore we used $[Mo_2(O_2CCMe_3)_2(NCMe)_4]^{2+}$ (**3b**) instead of **3a** as a starting material in order to achieve better solubility. Reactions of **2a**−**c** with **3b** in dichloromethane afforded the corresponding linear trinuclear complexes $[Mo_2PtX_2(pyphos)_2(O_2CCMe_3)_2]_2$ (**5a**, X = Cl; **5b**, X = Br; **5c**, X = I) in modest yields.

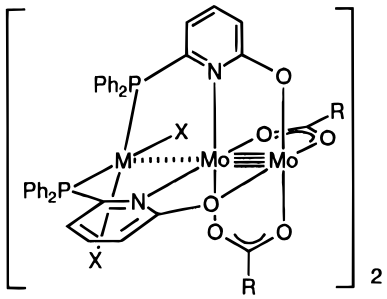

1: M = Pd, X = Cl, R = Me

4a: M = Pt, X = Cl, R = Me

4b: M = Pt, X = Br, R = Me

4c: M = Pt, X = I, R = Me

5a: M = Pt, X = Cl, R = CMe_3

5b: M = Pt, X = Br, R = CMe_3

5c: M = Pt, X = I, R = CMe_3

Crystal Structures of 4b and 5a−c. Crystal structures of the monomeric part of **5a** and the dimeric structure of **5b** are shown in Figures 1 and 2, respectively. Selected interatomic distances and angles of **4b** and **5a**−**c** are listed in Table 1. In these complexes, a platinum atom sits at an axial position of the Mo−Mo bond, and thus the three metal atoms, *i.e.* one Pt atom and two Mo atoms, are aligned linearly. Angles of Pt−Mo(1)−Mo(2) in complexes **4b** and **5a**−**c** range from 172.4 to 174.6°. Two *cis*-arranged pyphos ligands coordinate to the platinum atom by their phosphorus atoms and bridge the Mo_2 moiety by two N−O chelations. Two carboxylates also bridge the Mo_2 core in a *cis* fashion. The platinum atom in **4b** and **5a**−**c** is in square planar coordination environment composed of two *cis* halogen atoms and two *cis* phosphorus atoms of the pyphos ligands. The vector of the Mo−Mo bond in **4b** and **5a**−**c** is nearly perpendicular to each square plane; the angles

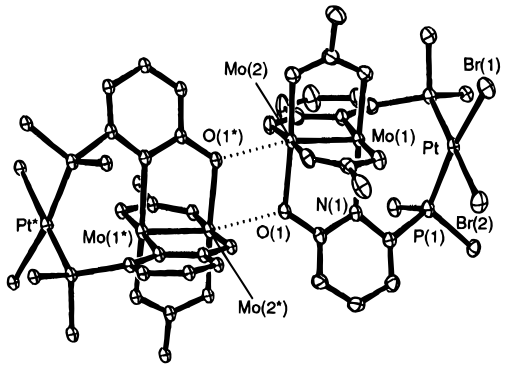

Figure 2. View of the dimeric structure of **5b** with labeling scheme. Phenyl groups bound to the phosphorus atom and *tert*-butyl groups are omitted for clarity. Thermal ellipsoids are drawn at the 30% probability level.

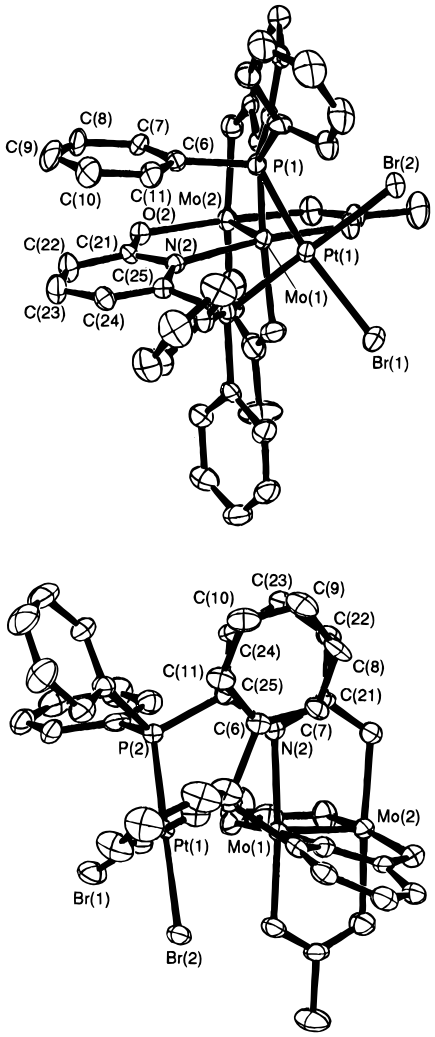

Figure 3. Molecular structure of **4b**: (a, top) side view; (b, bottom) top view. Thermal ellipsoids are drawn at the 30% probability level.

Mo(1)−Pt−P and Mo(1)−Pt−X (X = Cl, Br, I) deviate slightly acutely (maximum 7°) and obtusely (maximum 11°) from 90°, respectively. One phenyl ring of a pyphos ligand stacks on a pyridone ring of the other pyphos ligand, as shown in Figure 3. This is represented by the dihedral angles between the least-squares planes: **4b**, 10.59°; **5a**, 8.92°; **5b**, 13.37°; **5c**, 7.57°. The average distances from the phenyl ring to carbon atoms of the pyridone ring are 3.14 Å (**4b**), 3.21 Å (**5a**), 3.27 Å (**5b**), and 3.19 Å (**5c**), which are in the range of the ring stacking distances reported so far.[11−14]

The Mo−Mo bond distances in **4b** [2.096(1) Å], **5a** [2.094(1) Å], **5b** [2.0962(8) Å], and **5c** [2.1023(9) Å] are comparable

Table 1. Interatomic Distances (Å) and Angles (deg) for Complexes **4b** and **5a**−**c**[a]

	4b	5a	5b	5c
		Distances		
Mo(1)−Mo(2)	2.096(1)	2.094(1)	2.0962(8)	2.1023(9)
Mo(1)−Pt	3.001(1)	2.956(1)	2.9746(7)	3.0035(9)
Mo(1)−N(1)	2.21(1)	2.175(9)	2.208(6)	2.212(5)
Mo(1)−N(2)	2.209(9)	2.19(1)	2.173(6)	2.193(5)
Mo(1)−O(3)	2.124(9)	2.096(8)	2.107(5)	2.108(5)
Mo(1)−O(5)	2.125(8)	2.097(9)	2.101(5)	2.116(5)
Mo(2)−O(1)	2.074(9)	2.086(8)	2.078(5)	2.095(5)
Mo(2)−O(2)	2.096(7)	2.064(8)	2.055(5)	2.059(5)
Mo(2)−O(4)	2.108(9)	2.120(8)	2.073(5)	2.103(5)
Mo(2)−O(6)	2.113(9)	2.095(9)	2.116(5)	2.107(5)
Pt−X(1)	2.461(1)	2.342(3)	2.464(1)	2.6395(8)
Pt−X(2)	2.486(1)	2.322(4)	2.4771(9)	2.6687(7)
Pt−P(1)	2.254(3)	2.253(3)	2.259(2)	2.280(2)
Pt−P(2)	2.262(3)	2.244(3)	2.259(2)	2.265(2)
C(6)−N(2)	3.40(1)	3.53(2)	3.469(9)	3.448(9)
C(7)−C(21)	3.34(2)	3.61(2)	3.56(1)	3.53(1)
C(8)−C(22)	3.48(2)	3.68(3)	3.73(2)	3.60(1)
C(9)−C(23)	3.60(2)	3.67(3)	3.82(1)	3.53(1)
C(10)−C(24)	3.62(2)	3.66(3)	3.75(1)	3.50(1)
C(11)−C(25)	3.58(2)	3.59(2)	3.62(1)	3.51(1)
Mo(2)···Mo(2*)	3.880(2)	3.698(2)	3.708(1)	3.775(1)
		Angles		
Mo(2)−Mo(1)−Pt	172.40(5)	174.64(6)	173.66(3)	174.44(3)
Mo(2)−Mo(1)−N(1)	89.1(3)	91.2(2)	89.8(1)	90.3(1)
Mo(2)−Mo(1)−N(2)	92.0(2)	90.2(3)	91.4(1)	91.1(1)
Mo(2)−Mo(1)−O(3)	91.8(3)	91.3(2)	90.9(1)	90.9(1)
Mo(2)−Mo(1)−O(5)	90.0(5)	90.6(2)	92.0(1)	90.8(1)
Mo(1)−Mo(2)−O(1)	95.2(2)	93.2(2)	95.1(1)	94.1(1)
Mo(1)−Mo(2)−O(2)	92.3(2)	95.1(2)	93.6(1)	94.0(1)
Mo(1)−Mo(2)−O(4)	92.6(2)	91.5(2)	92.5(1)	92.6(1)
Mo(1)−Mo(2)−O(6)	93.5(2)	92.8(2)	91.2(1)	92.1(1)
Mo(1)−Pt−X(1)	99.48(5)	95.0(1)	97.73(3)	101.26(2)
Mo(1)−Pt−X(2)	94.57(4)	99.1(1)	96.60(3)	96.11(3)
Mo(1)−Pt−P(1)	84.18(8)	83.28(9)	84.18(5)	83.52(5)
Mo(1)−Pt−P(2)	84.39(7)	85.41(9)	83.18(5)	84.13(5)
Mo(1)−Mo(2)···Mo(2*)	124.20(5)	136.62(7)	135.92(3)	134.24(3)

[a] X denotes halogen atoms bound to platinum. X = Cl for **5a**, X = Br for **4b** and **5b**, and X = I for **5c**.

to those found for **1** [2.083(6) and 2.099(6) Å],[6] $Mo_2(pyphos)_4$ [2.098(2) Å],[15] and carboxylato-bridged Mo—Mo complexes such as $Mo_2(O_2CCH_3)_4$ [2.0934(8) Å][16] and $Mo_2(O_2CCMe_3)_4$ [2.096(1) and 2.087(1) Å].[2,17] These bond distances are slightly longer than that of the Mo−Mo bond supported by an O−N chelate ligand, as *e.g.* in $Mo_2(mhp)_4$ (where mhp represents the anion of 2-hydroxy-6-methylpyridine) [2.065(1) Å].[18]

The Pt−Mo(1) interatomic distances in complexes **5a**−**c** are 2.956(1), 2.9746(7), and 3.0035(9) Å, respectively, and are elongated according to the order of electronegativity of the halogen bound to platinum, Cl < Br < I. These distances suggest that the bonding between Pt and the Mo_2 core is weak. The Pt−Mo(1) distance of the acetato complex **4b** [3.001(1) Å] is 0.02 Å longer than that of the pivalato complex **5b**. They are both longer than the Pt−Mo single-bond distance of $(CO)_4Mo(\mu\text{-}PPh_2)_2Pt(PEt_3)$ [2.766(1) Å][9] and the Pd−Mo distance of $(\eta\text{-}C_5H_5)(CO)_2Mo(\mu\text{-}PCy_2)Pd(PCy_2H)_2$ (Cy = cyclohexyl) [2.916(2) Å].[19] No distinct difference is found between these Pt−Mo distances of **5a**−**c** and the Pd−Mo distances reported for **1** [3.025(6) and 2.976(6) Å]. The Pt−Mo distances of **4b** and **5a**−**c** are longer than the P···N distances [2.678(6)−2.77(1) Å], and this is responsible for the deviations of the dihedral angles between PtP_2X_2 planes and the MoN_2O_2 plane (**4b**, 16.2°; **5a**, 13.5°; **5b**, 14.2°; **5c**, 17.5°) from 0°.

Table 2. Selected Torsion Angles (deg) in **4b** and **5a**−**c**

	4b	5a	5b	5c
O(1)−Mo(2)−Mo(1)−N(1)	7.8(4)	4.0(5)	5.2(2)	5.3(2)
O(2)−Mo(2)−Mo(1)−N(2)	5.2(3)	3.4(3)	4.3(2)	3.5(2)
O(3)−Mo(1)−Mo(2)−O(4)	2.9(4)	1.4(4)	2.5(2)	3.1(2)
O(5)−Mo(1)−Mo(2)−O(6)	3.3(4)	1.1(3)	2.7(2)	2.5(2)
Mo(1)−Mo(2)··· Mo(2*)−Mo(1*)	133.55(7)	180.00	180.00	180.00

Chart 1

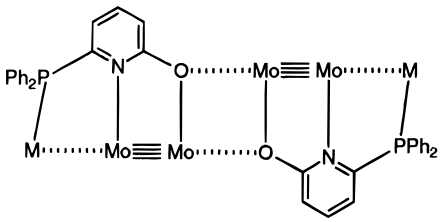

α

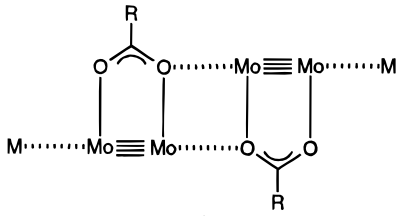

β

Torsion angles about the Mo−Mo axis are sensitive to the δ bonding of the Mo−Mo moiety.[20,21] The torsion angles of **4b** and **5a**−**c** are listed in Table 2. The averaged torsion angles of **4b** (average 4.8°), **5a** (average 2.5°), **5b** (average 3.7°), and **5c** (average 3.4°) are comparable to those of dinuclear complexes such as $Mo_2(pyphos)_4$ (average 0.5°) and $Mo_2(O_2CCMe_3)_4$ (average 0.4°,[2] average 0.1°,[17] and average 0.3°[17]), indicating that these linear trinuclear complexes maintain the quadruple bond.

The O(1) atom of the pyphos ligand in **4b** and **5a**−**c** is situated close to the Mo(2) atom of the neighboring molecule as shown in Figure 2, and thus these complexes have a dimeric structure (defined as the α form). It is noteworthy that the geometry of axial the Mo···O interaction in **4b** and **5a**−**c** is different from that of **1**, where the oxygen atom of a bridging carboxylate interacts with the adjacent Mo_2 moiety to form a dimeric structure (defined as the β form). These two forms of interaction are schematically shown in Chart 1. Complexes **4b** and **5a**−**c** have an α form interaction, and only complex **1** has a β form. The β form has usually been found in infinite structures of tetrakis(μ-carboxylato)dimolybdenum complexes[2,17] as well as in the dimeric structure around the Mo_2 core in $[Mo_2(O_2CCMe_3)_3]_2(\mu\text{-}2,7\text{-}O_2N_2C_8H_4)$.[5]

The axial Mo···O distances of **5** [**5a**, 2.570(8) Å; **5b**, 2.563(4) Å; **5c**, 2.568(4) Å] lie in the same range as those in **1** [2.55(3) and 2.56(3) Å]. These values are shorter by 0.3 Å than

(11) Miyamura, K.; Mihara, A.; Fujii, T.; Gohshi, Y.; Ishii, Y. *J. Am. Chem. Soc.* **1995**, *117*, 2377.
(12) Yamauchi, O.; Odani, A.; Masuda, H. *Inorg. Chim. Acta* **1992**, *198*−*200*, 749.
(13) Yamauchi, O.; Odani, A. *J. Am. Chem. Soc.* **1985**, *107*, 5938.
(14) Sugimori, T.; Shibakawa, K.; Masuda, H.; Odani, A.; Yamauchi, O. *Inorg. Chem.* **1993**, *32*, 4951.
(15) The structure of $Mo_2(pyphos)_4$ was confirmed by X-ray crystallography and will be reported elsewhere.
(16) Cotton, F. A.; Mester, Z. C.; Webb, T. R. *Acta Crystallogr.* **1974**, *B30*, 2768.
(17) Martin, D. S.; Huang, H.-W. *Inorg. Chem.* **1990**, *29*, 3674.
(18) Cotton, F. A.; Fanwick, P. E.; Niswander, R. H.; Sekutowski, J. C. *J. Am. Chem. Soc.* **1978**, *100*, 4725.
(19) Braunstein, P.; de Jésus, E.; Tiripicchio, A.; Camellini, M. T. *J. Organomet. Chem.* **1989**, *368*, C5.
(20) Cotton, F. A.; Feng, X. *J. Am. Chem. Soc.* **1993**, *115*, 1074.
(21) Cotton, F. A.; Eglin, J. L.; Hong, B.; James, C. A. *Inorg. Chem.* **1993**, *32*, 2104.

Scheme 1

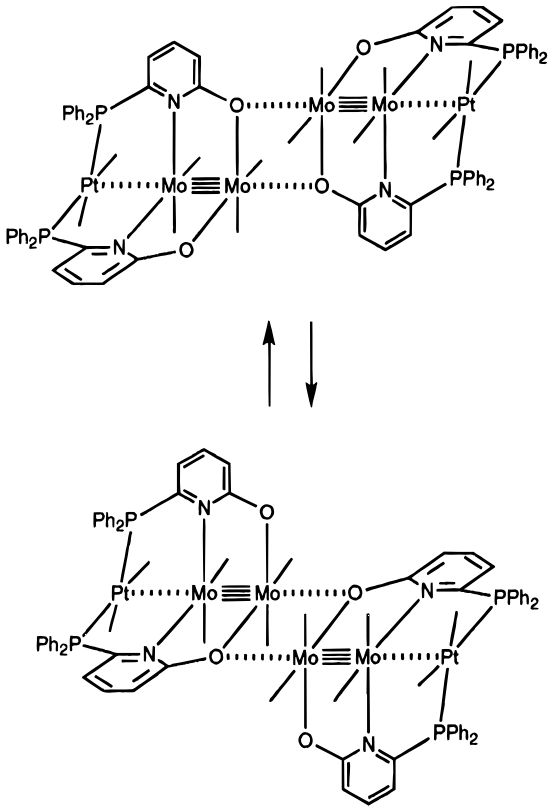

those of $Mo_2(O_2CCMe_3)_4$ [2.870(5) Å,[2] 2.894(5) Å,[17] and 2.905(5) Å[17]] and $[Mo_2(O_2CCMe_3)_3]_2(\mu$-2,7-$O_2N_2C_8H_4)$ [2.814(5) and 2.841(6) Å][5] and are also shorter than those of **4b** [2.631(8) Å] and $Mo_2(O_2CCH_3)_4$ [2.645(4) Å].[16]

The distances between the Mo(2) atom and the Mo(2*) atom of **4b** and **5** are 3.698(2)−3.880(2) Å, which are longer than that between internal Mo atoms [3.174(1) Å] of the Mo−Mo···Mo−Mo chain in $[Mo_2(O_2CCMe_3)_3]_2(\mu$-2,7-$O_2N_2C_8H_4)$[5] by 0.5−0.7 Å. The Mo(1)−Mo(2)···Mo(2*) angles [124.20(5)−136.62(7)°] are smaller than Mo−Mo···Mo in $[Mo_2(O_2CCMe_3)_3]_2(\mu$-2,7-$O_2N_2C_8H_4)$ (149°).[5] The twist angles between two Mo−Mo moieties of **4b** and **5** are listed in Table 2. Those of **5a**−**c** (180.00°) are different from that of **4b** [133.55(7)°].

Solution NMR Study of 5. The ^{1}H NMR spectrum of **5a** in dichloromethane-d_2 is temperature-dependent. At low temperature, there are two types of pivalato ligands in the integral ratio 1:1 assignable to carboxylates which are perpendicular to and in-plane with, respectively, the MoMo*OO* unit. The broadening occurs as the temperature rises to the coalescence point (T_c = 223 K). Above T_c, only one singlet resonance is observed, indicating the fluxionality of **5a**. All proton signals due to the two pyphos ligands exhibit behavior similar to that of the proton signals of the pivalato ligands. The fluxionality observed for **5a** is attributed to the rapid exchange of coordination site of adjacent molybdenum atoms; *i.e.*, the molybdenum atom slips from one oxygen atom to the other as shown in Scheme 1. The fluxionality is observed even in the coordinating solvent THF-d_8 (T_c = 233 K, $\Delta G^{\ddagger}$ = 47.9 kJ mol^{-1}). Thus, complex **5a** is found to have dimeric structure in solution though it has no bridging ligand between two Mo$\frac{4}{}$Mo moieties. Similar fluxionality was found in $[Mo_2(O_2CCMe_3)_3]_2(\mu$-2,7-$O_2N_2C_8H_4)$, where the two Mo$\frac{4}{}$Mo cores are bridged by a 2,7-dioxynaphthyridine ligand.[5] The ^{1}H NMR spectra of **5b** and **5c** are similar to that of **5a**. The T_c values and thermodynamic parameters of **5a**−**c** are listed in Table 3. The observed T_c value of each complex increases in the order of electronegativity of the halo ligands on the axial platinum atom. The electronic influence of the halo ligand on Pt affects the magnitude of an axial Mo···O interaction, which increases in the same order.

Table 3. Variable-Temperature ^{1}H NMR Spectral Data and Thermodynamic Parameters Calculated for the Fluxional Process of **5** in CD_2Cl_2

complex	δ(203 K)	$\Delta\nu$(203 K), Hz	T_c, K	$\Delta G^{\ddagger}$,[a] kJ mol^{-1}
5a	0.99 1.12	37	223	47.0
5b	1.00 1.12	33	238	50.6
5c	1.03 1.15	31	253	54.3

[a] $\Delta G^{\ddagger} = 8.314T_c[23.76 + \ln(T_c/k_c)]$ where $k_c = \pi(\Delta\nu)/2^{1/2}$.

This fluxionality of **5** is also observed in ^{31}P NMR spectroscopy. The ^{31}P{^{1}H} NMR spectrum of **5c** at 213 K displays two signals at δ 8.2 ($^2J_{P-P}$ = 6 Hz, $^1J_{Pt-P}$ = 2941) and 18.8 ($^2J_{P-P}$ = 6 Hz, $^1J_{Pt-P}$ = 3230 Hz) due to two different pyphos ligands. These two peaks broaden at 303 K; however, coalescence is not observed. Similar broadening is observed in the ^{31}P{^{1}H} NMR spectra of **5a** and **5b**; two separated signals at 213 K coalesce to one signal at 303 K. Because the time scale of ^{1}H NMR spectroscopy is shorter than that of ^{31}P NMR spectroscopy, the coalescence temperature of ^{31}P NMR will be higher than that of ^{1}H NMR.

Electronic Spectra. The absorption spectra of the linear trinuclear complexes **5a**−**c** exhibited strong bands at 424 nm (**5a**), 420 nm (**5b**), and 412 nm (**5c**). These absorptions can be ascribed to $\delta-\delta^*$ excitation on the quadruple Mo−Mo bond, since the λ_{max} values of **5** are similar to those of quadruply bonded dinuclear molybdenum complexes.[17,22−24] The observed absorption energies vary in the order I > Br > Cl, and the higher electronegativity at halogen results in lower absorption energy. As is evident from the X-ray study, the close contact between a platinum atom and a molybdenum atom only weakly transmits the electronic effect of halogen atoms to the orbitals at the Mo−Mo bond. The slight difference in the torsion angles about the Mo−Mo axis of **5a**−**c** makes it difficult to assess their influence on $\delta-\delta^*$ excitation.

Raman Spectra. The Raman spectrum of **5a** indicates ν(Mo−Mo) at 398 cm^{-1}, which is typical of the stretching of a strongly bonded Mo−Mo moiety with a quadruple bond. This value is comparable to those of Mo_2(pyphos)$_4$ (394 cm^{-1})[15] and $Mo_2(O_2CCH_3)_4$ (406 cm^{-1})[25−27] and is slightly lower in wavenumber than that of Mo_2(mhp)$_4$ (425 cm^{-1}).[18] The bromo and iodo derivatives **5b**,**c** show the same frequency (**5b**, 398 cm^{-1}; **5c**, 397 cm^{-1}). Thus the strongly bonded Mo−Mo moiety is insensitive to the delicate electronic effect on the platinum atom.[28]

Electrochemistry. We found that complexes **5a**−**c** are electrochemically similar to dinuclear Mo_2 complexes,[29] whose electrochemical processes have generally been described as one-electron processes due to redox at the filled δ-bonding orbital on the quadruple Mo−Mo bond. Cyclic voltammetries of **5a**−**c** were performed in dichloromethane, and the data were referred to Ag/AgCl. For complex **5c**, the representative cyclic vol-

(22) Cotton, F. A.; Martin, D. S.; Fanwick, P. E.; Peters, T. J.; Webb, T. R. *J. Am. Chem. Soc.* **1976**, *98*, 4681.
(23) Fanwick, P. E.; Martin, D. S.; Cotton, F. A.; Webb, T. R. *Inorg. Chem.* **1977**, *16*, 2103.
(24) Martin, D. S.; Newman, R. A.; Fanwick, P. E. *Inorg. Chem.* **1979**, *18*, 2511.
(25) San Filippo, J., Jr.; Sniadoch, H. J. *Inorg. Chem.* **1973**, *12*, 2326.
(26) Angell, C. L.; Cotton, F. A.; Frenz, B. A.; Webb, T. R. *J. Chem. Soc., Chem. Commun.* **1973**, 399.
(27) Trogler, W. C.; Solomon, E. I.; Trajberg, I.; Ballhausen, C. J.; Gray, H. B. *Inorg. Chem.* **1977**, *16*, 828.

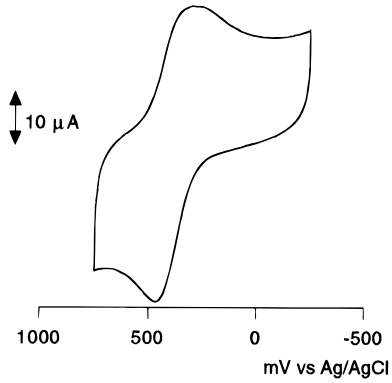

Figure 4. Cyclic voltammogram of **5b**.

Table 4. Electrochemical Data for **5a**−**c**[a]

complex	E_{red}, mV	E_{ox}, mV	$E_{1/2}$, mV	i_{pa}/i_{pc}
5a	150	280	220	0.6
5b	280	470	380	1.7
5c	380	490	430	1.2

[a] All compounds were studied as 1.0 mM solutions in dichloromethane containing 0.2 M tetra-*n*-butylammonium perchlorate as supporting electrolyte at a scan rate of 100 mV/s.

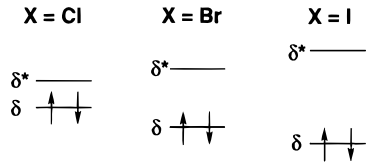

Figure 5. Energy level diagram for δ and δ^* of the Mo_2 core in complexes **5a**−**c**.

tammogram between −250 and +750 mV is shown in Figure 4, and the data for **5a**−**c** are summarized in Table 4. We observed a quasi-reversible process, corresponding to one-electron oxidation of the filled δ-bonding orbital on the Mo−Mo bond. The variation of halo ligands on a platinum atom provided information about the relative energy level of the filled δ orbital. The observed $E_{1/2}$ values of **5a**−**c** indicate the δ level (HOMO) in the order Cl > Br > I.

Conclusion

We have found that a platinum(II) moiety can be placed at an axial position of a Mo_2 core by using tridentate pyphos ligands to form linear trinuclear complexes, **4** and **5**. Crystallographic study revealed that **5a**−**c** have almost the same Mo−Mo bond distances. In contrast, the electronic absorption spectra and cyclic voltammograms depend on the halogen atom attached to platinum. The less electronegative halogen atom bound to the platinum atom causes the energy level of the δ orbital to lower. The $\delta-\delta^*$ gap is schematically shown in Figure 5.

The interatomic distances between the Pt(II) atom and the Mo atom are thus found to be too long to be regarded as single bonds. In these complexes, the Pt···Mo interaction is under the influence of the halo ligands on the platinum atom and the alkyl group of the equatorial carboxylato ligand, whereas the Mo−Mo distance is not affected by these substitutions.

Experimental Section

General Procedures. All manipulations were carried out by the use of standard Schlenk techniques under argon atmosphere. All solvents were purified by distillation under argon after drying over calcium hydride or sodium benzophenone ketyl. Complex **3**, $[Mo_2(O_2CCR_3)_2(NCCH_3)_6](BF_4)_2$ (**a**, R = H;[30] **b**, R = CH_3[5]), and 6-(diphenylphosphino)-2-pyridone[31] were prepared according to the literature.

Physical Measurements. Nuclear magnetic resonance (^{1}H, ^{31}P NMR) spectra at 303 K were measured on a JEOL JNM-GSX-270 (^{1}H, 270 MHz; ^{31}P, 109 MHz) spectrometer, and variable-temperature ^{1}H and ^{31}P NMR spectra were obtained on JEOL JNM-EX-270 (^{1}H, 270 MHz) and JEOL JNM-LA-500 (^{31}P, 202 MHz) spectrometers, respectively. The ^{31}P NMR spectrum of **5c** at 303 K was measured on a JEOL JNM-GSX-400 (^{31}P, 162 MHz) spectrometer. All ^{1}H NMR chemical shifts were reported in ppm relative to protio impurity resonance as follows: chloroform-*d*, singlet at 7.27 ppm; dichloromethane-d_2, triplet at 5.32 ppm; THF-d_8, broad singlet at 3.60 ppm (−O−CDH−CD_2−). ^{31}P NMR chemical shifts were reported in ppm relative to an external reference of 85% H_3PO_4 at 0.00 ppm. Mass spectra were recorded on a JEOL SX-102 spectrometer. Raman spectra were recorded at 298 K on a Jasco R-800 spectrometer equipped HTV-R649 photomultiplier with Ar^+ laser excitation (514.5 nm) using KBr disk samples sealed in glass tubes under argon atmosphere. Elemental analyses were performed at the Elemental Analysis Center of Osaka University. UV−vis spectra were taken on a Shimadzu UV-3100 spectrometer in a sealed 1 mm cell. All melting points were measured in sealed tubes and were not corrected.

Preparation of $PtCl_2$(pyphosH)$_2$ (2a). A mixture of $PtCl_2(cod)_2$ (0.257 g, 0.687 mmol) and pyphosH (0.383 g, 1.37 mmol) in dichloromethane (40 mL) was stirred at room temperature for 1 day. All the volatiles were removed, and the resulting solid was washed with diethyl ether to afford quantitatively a white powder of **2a**, mp 235−240 °C dec. ^{1}H NMR ($CDCl_3$, 303 K): δ 6.49 (t, 2H), 6.73 (d, 2H), 7.20−7.59 (m, 24H). ^{31}P{^{1}H} NMR ($CDCl_3$, 303 K): δ 12.6 (s, J_{Pt-P} = 3592 Hz). Anal. Calcd for $C_{34}H_{28}N_2O_2P_2PtCl_2$: C, 49.53; H, 3.42; N, 3.40. Found: C, 50.01; H, 3.85; N, 2.97.

$PtBr_2$(pyphosH)$_2$ (**2b**) and PtI_2(pyphosH)$_2$ (**2c**) were prepared similarly to **2a**.

2b: yellowish white powder; quantitative yield; mp 248−252 °C dec. ^{1}H NMR ($CDCl_3$, 303 K): δ 6.52 (t, 2H), 6.73 (d, 2H), 7.20−7.61 (m, 24H). ^{31}P{^{1}H} NMR ($CDCl_3$, 303 K): δ 11.4 (s, J_{Pt-P} = 3533 Hz). Anal. Calcd for $C_{34}H_{28}N_2O_2P_2PtBr_2$: C, 44.71; H, 3.09; N, 3.09. Found: C, 44.07; H, 3.11; N, 2.25.

2c: yellow powder; quantitative yield; mp 247−251 °C dec. ^{1}H NMR ($CDCl_3$, 303 K): δ 6.55 (m, 2H), 6.71 (d, 2H), 7.20−7.63 (m, 24H). ^{31}P{^{1}H} NMR ($CDCl_3$, 303 K): δ 7.8 (s, J_{Pt-P} = 3381 Hz). Anal. Calcd for $C_{34}H_{28}N_2O_2P_2PtI_2(CH_2Cl_2)_{0.5}$: C, 39.47; H, 2.78; N, 2.67. Found: C, 39.52; H, 2.98; N, 2.52.

Preparation of $[Mo_2PtCl_2$(pyphos)$_2(O_2CCH_3)_2]_2$ (4a). To a mixture of $Mo_2(O_2CCH_3)_4$ (53 mg, 0.124 mmol) and **3a** (90 mg, 0.124 mmol) in dichloromethane (30 mL) was added **2a** (202 mg, 0.245 mmol). The reaction mixture was stirred for 12 h at room temperature. The precipitated solids were removed by filtration. The supernatant was concentrated, and then crystallization of the resulting solid from a mixture of dichloromethane and diethyl ether afforded **4a** as dark red crystals (56% yield), mp >300 °C. Once isolated, complex **4a** has low solubility, and further spectroscopic characterization was not possible. The reaction of **2a** (103 mg, 0.125 mmol) with **3a** (69 mg, 0.095 mmol) gave **4a** (5.6 mg) in 5% yield. Anal. Calcd for $C_{38}H_{32}Cl_2N_2O_6P_2Mo_2Pt(CH_2Cl_2)$: C, 38.48; H, 2.81; N, 2.30. Found: C, 38.52; H, 2.81; N, 2.30.

Complexes **4b**,**c** were prepared similarly to **4a**.

4b: dark red crystals; 44% yield; mp >300 °C. Anal. Calcd for $C_{38}H_{32}Br_2N_2O_6P_2Mo_2Pt(CH_2Cl_2)$: C, 35.86; H, 2.62; N, 2.14. Found: C, 35.72; H, 2.60; N, 2.18.

(28) In the case of **5b**, ν(Mo−Mo) was observed at 398 cm^{-1} accompanied by that of the photoreduction product at 382 cm^{-1}. Similar reduction was observed in the Raman spectrum of the platinum(II) complex $Mo_2Pt^{II}_2Br_4$(pyphos)$_4$, where ν(Mo−Mo) at 395 cm^{-1} was observed together with that of the Pt−Mo bonded platinum(I) complex $Mo_2Pt_2Br_2$(pyphos)$_4$ at 382 cm^{-1}. This would indicate that photoreduction of **5b** afforded a Pt−Mo bonded complex, which will be an object of further research. The study of tetranuclear complexes will be reported elsewhere.

(29) Chisholm, M. H.; Clark, D. L.; Huffman, J. C.; Van Der Sluys, W. G.; Kober, E. M.; Lichtenberger, D. L.; Bursten, B. E. *J. Am. Chem. Soc.* **1987**, *109*, 6796.

(30) Cotton, F. A.; Reid, A. H., Jr.; Schwotzer, W. *Inorg. Chem.* **1985**, *24*, 3965.

(31) Newkome, G. R.; Hager, D. C. *J. Org. Chem.* **1978**, *43*, 947.

Table 5. Crystallographic Data for **4b** and **5a**−**c**

complex	**4b**	**5a**	**5b**	**5c**
empirical formula	$C_{42}H_{40}Cl_8Br_2Mo_2N_2O_6P_2Pt$	$C_{45}H_{46}Cl_4Mo_2N_2O_6P_2Pt$	$C_{45}H_{46}Br_2Cl_2Mo_2N_2O_6P_2Pt$	$C_{45}H_{46}Cl_2I_2Mo_2N_2O_6P_2Pt$
fw	1561.14	1301.60	1390.50	1484.5
space group	*C*2/*c* (No. 15)	$P\bar{1}$ (No. 2)	$P\bar{1}$ (No. 2)	$P2_1/n$ (No. 14)
a, Å	34.733(4)	13.541(3)	12.211(2)	13.359(4)
b, Å	17.81(1)	17.029(3)	20.859(3)	19. 686(3)
c, Å	22.530(5)	12.896(3)	10.478(2)	20.392(4)
α, deg		101.20(2)	98.88(1)	
β, deg	124.444(8)	117.00(1)	112.55(2)	107.92(2)
γ, deg		85.47(2)	84.56(1)	
Z	8	2	2	4
V, Å^3	11498(5)	2599(1)	2433.3(8)	5101(2)
d_{calcd}, g cm^{-3}	1.830	1.663	1.898	1.993
λ(MoKα), Å	0.710 69	0.71069	0.71069	0.71069
abs coeff, cm^{-1}	47.09	33.54	52.33	46.70
temp, °C	23	23	23	23
R^a	0.060	0.050	0.042	0.039
$R_w{}^b$	0.084	0.064	0.049	0.031

^{a} $R = \sum||F_o| - |F_c||/|F_o|$. ^{b} $R_w = [\sum w(|F_o| - |F_c|)^2/\sum wF_o^2]^{1/2}$; $w = 1/\sigma^2(F_o)$. Function minimized: $\sum w(|F_o| - |F_c|)^2$.

4c: dark red crystals; 59% yield; mp >300 °C. Anal. Calcd for $C_{38}H_{32}I_2N_2O_6P_2Mo_2Pt(CH_2Cl_2)$: C, 33.45; H, 2.45; N, 2.00. Found: C, 33.87; H, 2.48; N, 2.07.

Preparation of $[Mo_2PtCl_2(pyphos)_2(O_2CCMe_3)_2]_2$ (5a). Complexes **3b** (424 mg, 0.512 mmol) and **2a** (441 mg, 0.535 mmol) were dissolved in dichloromethane (40 mL). After the reaction mixture was stirred for 3 days at 30 °C, the precipitated solids were removed by filtration. The supernatant was concentrated, and crystallization of the resulting solid from a mixture of dichloromethane and diethyl ether afforded **5a** as dark red crystals (45% yield), mp >300 °C. ^{1}H NMR (CD_2Cl_2, 303 K): δ 1.22 (s, 18H), 6.58 (br s, 2H), 6.85 (brs, 4H), 6.20−7.56 (m, 20H). ^{1}H NMR (THF-d_8, 303 K): δ 1.15 (s, 18H), 6.52 (brs, 2H), 6.86 (brs, 4H), 7.17 (brs, 8H), 7.32 (brs, 8H), 7.40 (brs, 8H). ^{31}P{^{1}H} NMR (CD_2Cl_2, 303 K): δ 18.3 (brs, J_{Pt-P} = 3288 Hz). ^{31}P{^{1}H} NMR (CD_2Cl_2, 213 K): δ 14.9 (s), δ 20.6 (s). UV−vis (CH_2Cl_2), λ_{max}, nm (ϵ, M^{-1} cm^{-1}): 424 (2.5 × 10^3). Raman, ν(Mo−Mo): 398 cm^{-1}. FAB mass spectrum *m*/*z*: 1216 (M$^+$). Anal. Calcd for $C_{44}H_{44}N_2O_6P_2Mo_2PtCl_2(CH_2Cl_2)$: C, 41.53; H, 3.56; N, 2.15. Found: C, 41.59; H, 3.71; N, 2.65.

Complexes **5b,c** were prepared similarly.

5b: dark red crystals; yield 53%; mp >300 °C. ^{1}H NMR (CD_2Cl_2, 303 K): δ 1.16 (s, 18H), 6.59 (brs, 2H), 6.83 (brs, 4H), 7.21−7.55 (m, 20H). ^{31}P{^{1}H} NMR (CD_2Cl_2, 303 K): δ 17.1 (br s, J_{Pt-P} = 3230 Hz). ^{31}P{^{1}H} NMR (CD_2Cl_2, 213 K): δ 13.1 (s, J_{Pt-P} = 3116 Hz), 20.39 (s, J_{Pt-P} = 3395 Hz). UV−vis (CH_2Cl_2), λ_{max}, nm (ϵ, M^{-1} cm^{-1}): 420 (1.3 × 10^3). Raman, ν(Mo−Mo): 398 cm^{-1}. FAB mass spectrum *m*/*z*: 1307 (MH$^+$). Anal. Calcd for $C_{44}H_{44}N_2O_6P_2Mo_2PtBr_2$: C, 40.48; H, 3.40; N, 2.15. Found: C, 40.05; H, 3.31; N, 2.14.

5c: dark red crystals; yield 10%; mp >300 °C. ^{1}H NMR (CD_2Cl_2, 303 K): δ 1.19 (s, 18H), 6.82 (brs, 6H), 7.28 (br s, 12H), 7.40 (br s, 8H). ^{31}P{^{1}H} NMR (20% $CDCl_3$ in dichloromethane, 303 K): δ 8.5 (br s), 16.1 (br s). ^{31}P{^{1}H} NMR (CD_2Cl_2, 213 K): δ 8.2 (s, J_{Pt-P} = 2941 Hz, J_{P-P} = 6 Hz), 18.0 (s, J_{Pt-P} = 3230 Hz, J_{P-P} = 6 Hz). UV−vis (CH_2Cl_2), λ_{max}, nm (ϵ, M^{-1} cm^{-1}): 412 (1.3 × 10^3). Raman, ν-(Mo−Mo): 397 cm^{-1}. FAB mass spectrum *m*/*z*: 1400 (M$^+$). Anal. Calcd for $C_{44}H_{44}N_2O_6P_2Mo_2PtI_2(CH_2Cl_2)$: C, 36.41; H, 3.12; N, 1.89. Found: C, 36.17; H, 3.13; N, 1.93.

Cyclic Voltammetry of Complexes 5a−c. Cyclic votammograms were recorded with a BAS 100B electrochemical workstation referenced to a Ag/AgCl electrode. The working electrode was a glassy-carbon electrode, and the counter electrode was a platinum wire. The measurements were recorded on a 1.0 mM dichloromethane solution that contained 0.2 M tetra-*n*-butylammonium perchlorate as supporting electrolyte at the scan rate of 100 mV/s. Under our experimental conditions, the ferrocenium/ferrocene couple was observed at $E_{1/2}$ = 520 mV vs Ag/AgCl.

Crystallographic Data Collections and Structure Determinations for 4b and 5a−c. Data Collection. Each suitable crystal was mounted in a glass capillary under an argon atmosphere. Data for the four complexes were collected by a Rigaku AFC-5R diffractometer with graphite-monochromated Mo Kα radiation and a 12 kW rotating anode generator. The incident-beam collimator was 1.0 mm, and the crystal to detector distance was 285 mm. Cell constants and an orientation matrix for data collection, obtained from a least-squares refinement using the setting angles of 25 carefully centered reflections in the ranges 27.27° < 2θ < 32.52° for **4b**, 49.55° < 2θ < 53.89° for **5a**, 29.85° < 2θ < 29.97° for **5b**, and 35.11° < 2θ < 39.54° for **5c**, corresponded to the cells with dimensions listed in Table 5, where details of the data collection are summarized. The weak reflections [$I < 10\sigma(I)$] were rescanned (maximum of five rescans), and the counts were accumulated to ensure good counting statistics. Stationary-background counts were recorded on each side of the reflection. The ratio of peak counting time to background counting time was 2:1. Three standard reflections were chosen and monitored every 150 reflections.

Data Reduction. An empirical absorption correction based on azimuthal scans of several reflections was applied which resulted in transmission factors in the ranges 0.61−1.00 (for **4b**), 0.76−1.00 (for **5a**), 0.70−1.00 (for **5b**), and 0.60−1.00 (for **5c**). The data were corrected for Lorentz and polarization effects.

Structure Determination and Refinement. The structure of **5a** was solved by direct methods, SHELXS86,[32] and expanded using Fourier techniques. The structures of **4b**, **5b**, and **5c** were solved by heavy-atom Patterson methods, PATTY,[33] and expanded using Fourier techniques. Measured nonequivalent reflections with $I > 3.0\sigma(I)$ were used for the structure determination. The non-hydrogen atoms were refined anisotropically. The crystals of **5b** and **5c** each contain one solvent molecule, CH_2Cl_2, at definite positions. The CH_2Cl_2 molecule in the crystal of **5a** was found to be disordered at three different places. Four molecules of CH_2Cl_2 were disordered at five definite positions in the crystals of **4b**. In the final refinement cycle, coordinates of the hydrogen atoms were included at idealized positions and each hydrogen was assigned the same temperature factor as that of the carbon atom to which it was bonded. All calculations were performed using the teXsan crystallographic software package of the Molecular Structure Corp.

Acknowledgment. A.N. and K.M. are grateful for financial support from the Ministry of Education, Science and Culture of Japan (Specially Promoted Research Grant No. 06101004 and Grant-in-Aid for Developmental Scientific Research No. 07216249).

Supporting Information Available: Fully labeled ORTEP diagrams and tables giving X-ray experimental details and refinement parameters, bond lengths, bond angles, nonbonded contacts, least-squares planes, and final positional parameters and thermal parameters for **4b**, **5a**, **5b**, and **5c** (60 pages). Ordering information is given on any current masthead page.

IC950988B

(32) Sheldrick, G. M. *Crystallographic Computing 3*; Oxford University Press: Oxford, U.K., 1985; pp 175−189.

(33) Beurskens, P. T.; Admiraal, G.; Beurskens, G.; Bosman, W. P.; Garcia-Granda, S.; Gould, R. O.; Smits, J. M. M.; Smykalla, C. The DIRDIF program system. Technical Report of the Crystallography Laboratory; University of Nijmegen: Nijmegen, The Netherlands, 1992.